2010

Numerical Study of Air Inside Refrigerating Compartment of Frost-free Domestic Refrigerators

Julian Jaramillo
CTTC - UPC

Joaquim Rigola
CTTC - UPC

Carlos Pérez-Segarra
CTTC - UPC

Carles Oliet
CTTC - UPC

Numerical Study of Air inside Refrigerating Compartment of Frost-Free Domestic Refrigerators

Julian JARAMILLO[1,2], Joaquim RIGOLA[1], Carlos PEREZ-SEGARRA[1]*, Carles OLIET[1]

[1]Centre Tecnològic de Transferència de Calor (CTTC)
Universitat Politècnica de Catalunya (UPC)
ETSEIAT, C. Colom 11, 08222 Terrassa (Barcelona), Spain
Tel. +34-93-739.81.92, Fax: +34-93-739.89.20
cttc@cttc.upc.edu, http://www.cttc.upc.edu

[2]Institute of Mathematics and Computing Science, University of Groningen
P.O. Box 800, 9700 AV Groningen, The Netherlands

ABSTRACT

This paper is focussed on the study of the temperature and air distribution inside household frost-free refrigerators. It is well known that the correct air and temperature distribution inside the refrigerated chamber is the most important factor that affects refrigerator efficiency. In frost-free refrigerators the cooled air is supplied directly inside the fresh food and vegetable cabinets. Therefore, studies intended to establish the actual air flow and temperature distributions inside these cabinets are relevant in order to improve temperature homogeneity and to reduce energy consumption. The proposed methodology is based on the numerical simulation of the cabinets by means of computational fluid dynamics. Turbulence is solved by means of LES models. Unsteady three-dimensional numerical studies are carried out, simulating the cooling process starting from a uniform warm temperature inside the refrigerator. Furthermore, the influence of inlet and outlet ports location is also investigated.

1. INTRODUCTION

Nowadays, final users are not only concerned about the refrigerator capability to preserve perishable food products fresh, which is its basic function, but also about the refrigerator performance referring to energy saving (Fukuyo et al., 2003). It is well known that the correct air and temperature distribution inside the refrigerated chamber is the most important factor that affects refrigerator efficiency (Meng and Yu, 2009). Furthermore, a rapid cooling is also desirable to avoid a premature deterioration of the food products (Gupta et al., 2007). In frost-free refrigerators the cooled air is supplied directly inside the fresh food and vegetable cabinets. Therefore, studies intended to establish the actual air flow and temperature distributions inside these cabinets are relevant in order to improve temperature homogeneity and reduce energy consumption. Hence, this paper is focussed on the study of temperature and air distribution inside household frost-free refrigerators.

Household frost-free refrigerators have been working the last two decades. However, only a few studies dealing with the thermo-fluid dynamic behaviour inside this kind of refrigerators can be found in the technical literature. An example of the experimental work carried out to study the performance of the supply-air openings is that recently presented by Meng and Yu(Meng and Yu, 2009). Numerical studies to model refrigerator behaviour assuming steady state and laminar regime have been done by Gupta et al.(Gupta et al., 2007). They also conducted experiments to validate numerical results. They found a qualitative agreement between numerical and experimental results. Moreover, Fukuyo et al.(Fukuyo et al., 2003) and Ding et al.(Ding et al., 2004) solved turbulence by means of RANS $k-\epsilon$ models. Unlike, these papers, in this work turbulence is solved by means of advanced LES models. Furthermore, unsteady three-dimensional numerical studies, simulating the cooling process starting from a uniform warm temperature inside the refrigerator are carried out. Moreover, the influence of inlet and outlet ports location is considered.

The numerical methodology applied in the present paper is based on finite volume techniques. Governing partial differential equations are converted into algebraic ones using unstructured meshes. Second-order schemes are used for transient and spatial discretization. Local grid refinement is used(Lehmkuhl et al., 2007). Furthermore, the mathematical formulation used in this work is based on symmetry-preserving discretization of the governing equations, which assures that some important properties of the Navier-Stokes equations are retained in the discretization process(Verstappen and Veldman, 2003).

2. MATHEMATICAL FORMULATION

The volume-filtered Navier-Stokes equations of the fluid flow (continuity, momentum and energy), used in LES simulations, can be written as follows:

$$\frac{\partial \bar{u}_i}{\partial x_i} = 0 \tag{1}$$

$$\frac{\partial \bar{u}_i}{\partial t} + \bar{u}_j \frac{\partial \bar{u}_i}{\partial x_j} = -\frac{1}{\rho}\frac{\partial \bar{p}}{\partial x_i} + \frac{\partial}{\partial x_j}\left(2\nu \overline{S}_{ij} - \tau_{ij}\right) - \rho g_i \beta(\bar{T} - T_{ref}) \tag{2}$$

$$\frac{\partial \bar{T}}{\partial t} + \bar{u}_i \frac{\partial \bar{T}}{\partial x_i} = \frac{\partial}{\partial x_i}\left(\frac{\lambda}{\rho c_p}\frac{\partial \bar{T}}{\partial x_i} - h_i\right) \tag{3}$$

where h_i is the subgrid heat flux; and τ_{ij} is the subgrid stress tensor. The last one is generally modeled using the strain rate tensor of the resolved field $\overline{S}_{ij} = \frac{1}{2}\left(\frac{\partial \bar{u}_i}{\partial x_j} + \frac{\partial \bar{u}_j}{\partial x_i}\right)$, and the subgrid eddy viscosity, ν_{sgs}, as follows:

$$\tau_{ij} = \overline{u_i u_j} - \bar{u}_i \bar{u}_j = -2\nu_{sgs}\overline{S}_{ij} + \frac{1}{3}\tau_{kk}\delta_{ij} \tag{4}$$

Different models, which are explained below, can be used to model the subgrid eddy viscosity. Furthermore, for h_i the models use the simple eddy diffusivity approach that can be written as:

$$h_i = -\frac{\nu_{sgs}}{Pr_{sgs}}\frac{\partial \bar{T}}{\partial x_i} \tag{5}$$

where Pr_{sgs} is the subgrid Prandtl number.

2.1 Subgrid-scale model

A suitable approach for the subgrid eddy viscosity is needed to model turbulent scales which can not be resolved. The simplest model is the Smagorinsky model(Smagorinsky, 1963). In Smagorinsky's model, subgrid viscosity is proportional to the subgrid characteristic length scale Δ and to a characteristic turbulent velocity.

$$\nu_{sgs} = (C_s\Delta)^2\sqrt{2\bar{S}_{ij}\bar{S}_{ij}} \equiv (C_s\Delta)^2|\bar{S}| \tag{6}$$

A shortcoming of this model is that the Smagorinsky coefficient C_s is a constant that must be tunned. Furthermore, this model needs a damping function to correct the near-wall behaviour of the subgrid viscosity. Therefore, in order to overcome these deficiencies Nicoud and Ducros(Nicoud and Ducros, 1999) proposed a model known as wall adapting local eddy viscosity (WALE) model. This model accounts for the effects of both the strain and the rotation rate of the smallest resolved turbulent fluctuations. Moreover, it reproduces correctly the subgrid eddy viscosity behaviour near solid walls, and it does not require a second filtering operation to evaluate Smagorinsky coefficient. Therefore, WALE model, which is selected in this work to approximate subgrid eddy viscosity, reads:

$$\nu_{sgs} = (C_w\Delta)^2\frac{(\bar{S}^d_{ij}\bar{S}^d_{ij})^{3/2}}{(\bar{S}_{ij}\bar{S}_{ij})^{5/2}+(\bar{S}^d_{ij}\bar{S}^d_{ij})^{5/4}} \tag{7}$$

$$\bar{S}^d_{ij} = \frac{1}{2}(g^2_{ij} + g^2_{ji}) - \frac{1}{3}\delta_{ij}g^2_{kk},$$

$$g_{ij} = \frac{\partial \bar{u}_i}{\partial x_j}, \qquad g^2_{ij} = g_{ik}g_{kj},$$

$$C_w = 0.33 \qquad Pr_{sgs} = 0.4$$

3. NUMERICAL METHODOLOGY

The proposed methodology is based on the numerical simulation of the cabinets by means of computational fluid dynamics and heat transfer (CFD&HT). A new general purpose CFD&HT code, called TermoFluids(Lehmkuhl et al., 2007), is used in this work. The code uses efficient algorithms, which work adequately on slow networks of personal computers clusters. At is was commented, turbulence is solved by means of LES models(Sagaut, 2001). Governing partial differential equations are converted into algebraic ones using unstructured collocated meshes, symmetry-preserving discretization(Verstappen and Veldman, 2003), and considering Boussinesq assumption. Pressure-velocity coupling is solved by means of fully explicit fractional step algorithm. A third-order gear like scheme is used for time integration(Fishpool and Leschziner, 2009). Conservative schemes, which preserve kinetic energy, are applied for the spatial discretization. Local refinement of the grid, where large thermal and velocity gradients exist, is applied. Partitioning of the computational domain is carried out by means of MeTIS software. For the solution of the pressure (Poisson) equation, an iterative conjugate-gradient (CG) method with a diagonal scaling preconditioner is used(Borrell et al., 2007).

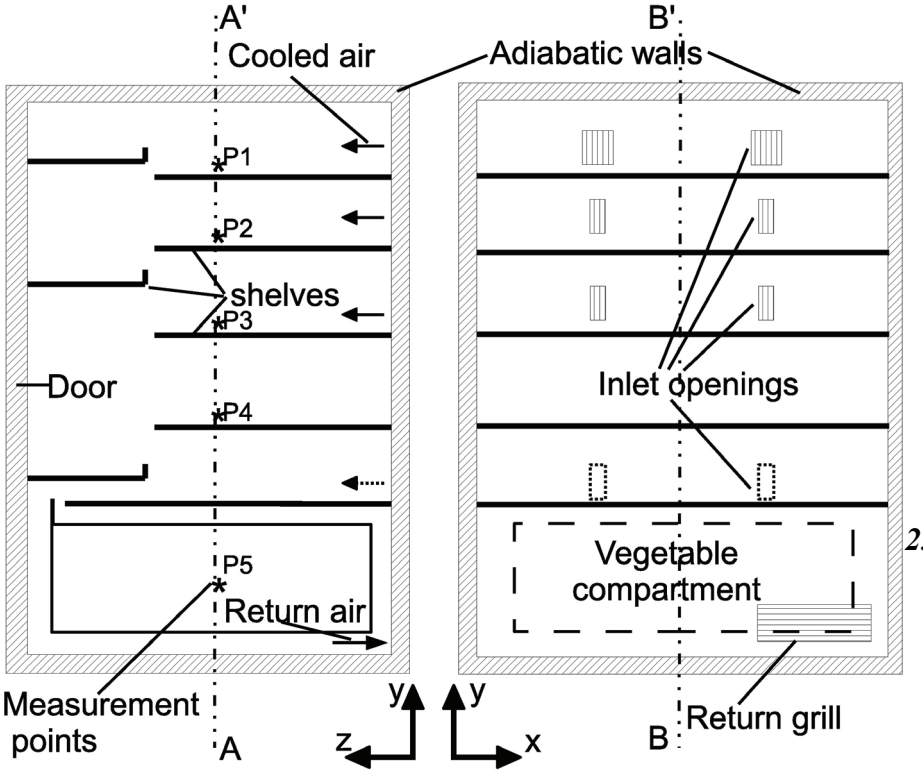

2378, Page 1

Figure 1: Refrigerator layout.

4. ILLUSTRATIVE NUMERICAL RESULTS

4.1 Configuration analysed

In Figure 1 a schematic representation of the refrigerating compartment studied is presented. The first $15s$ of the cooling process starting from a uniform warm temperature inside the refrigerator is numerically studied. At the beginning of the simulation a constant temperature of $283K$ is assumed in the whole space for the cases analysed. Uniform velocity and temperature profiles of cooled air are given at the inlet openings, which are located in the rear wall. An inlet mass flow rate of $2.0 \times 10^{-3} kg/s$ at $263K$ is imposed. Non-slip condition is used at walls and shelves. Furthermore, they are considered adiabatic. In the air return grill a pressure outflow boundary condition is assumed. Moreover, two inlet ports distributions are studied while inlet mass flow rate is kept constant.

Firstly, inlet openings plotted with solid line are used (referred as *case*1). Then, two inlet openings are added, which are depicted with dashed line in Figure 1 (referred as *case*2). Return grill, which is placed behind vegetable compartment, and the rest of the geometry is similar for the two cases. A fully three dimensional unstructured grid with approximately 4100000 control volumes is used. It is densified near air inlet, outlet and solid walls, taking care to capture steep gradients near these places.

4.2 Results and discussion

This section is dedicated to the presentation of numerical results obtained by the authors in order to characterise fluid-dynamic and thermal fields of the refrigerating compartment of a household frost-free refrigerator. Even tough the grid used for this simulation can be considered adequate, it is still advisable to carry out a more detailed verification process to determine the numerical results grid independence. However, given the complexity of the studied configuration a compromise between computational time and desired accuracy should be achieved. Therefore, results hereafter presented should be taken as a qualitative approximation.

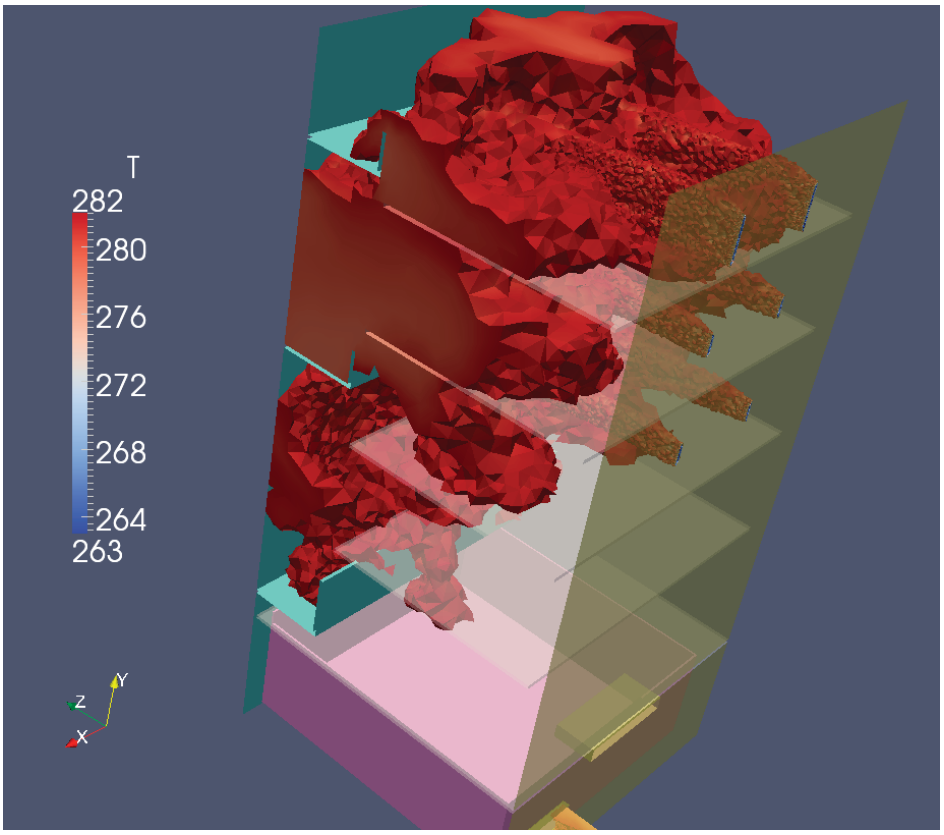

Figure 2: *case*1. Temperature distribution after 15s of cooling process starting.

Firstly, the geometry with six inlet openings, *case*1, is analysed. Numerical results for this configuration are presented in Figure 2. In this Figure, temperature distribution after 15s is shown. Red colour represents profiles where temperature has decreased one degree, i.e. air is at 9^oC. As it can be seen, in some regions temperature have not diminished even by 1^oC after 15s. Air flow in this refrigerating compartment is given by mixed convection. At the beginning, the air flows into the space impinging the door shelves. Then, part of it gains heat from the surroundings, becoming lighter and flowing up due to buoyancy effects. Straight after, recirculating it mixes with the cold air stream emanating from the inlets and flows down, entering the second shelve. At this point, part of the air settle down in the upper part of this space. Whereas, the other part is recirculated when it mixes with the inlet stream of this shelf. Finally, the combined air flows down

through the gap between the door and the shelf. The process is repeated for the third shelf. However, below the fourth shelf there are not inlet openings and most of the air is heated by the surroundings here and it creates a recirculation. Only a small part of the cold air flows down towards the lid of vegetable compartment.

In an effort to improve temperature and air distribution homogeneity in vertical direction, two new inlet openings are included below the fourth shelf from the top. Their location is depicted with dashed line in Figure 1 (*case*2). Mass flow is kept constant and similar to the one used in *case*1 configuration.
The most remarkable difference can be observed near the bottom part of the cabinet in Figure 3. As a consequence of the new inlet ports, cooled air now produces a decrease of the temperature near the vegetable compartment and the speace below fourth shelf, where the new inlets are located. Furthermore, in this Figure is easy to see that the temperature has reduced below, in the front of, and around the vegetable compartment. However, cooled air has not been introduced within vegetable box. Moreover, it seems that due to the new inlet velocity, the air temperature in the top part of the refrigerating compartment has decreased in *case*2 a bit more than in *case*1.

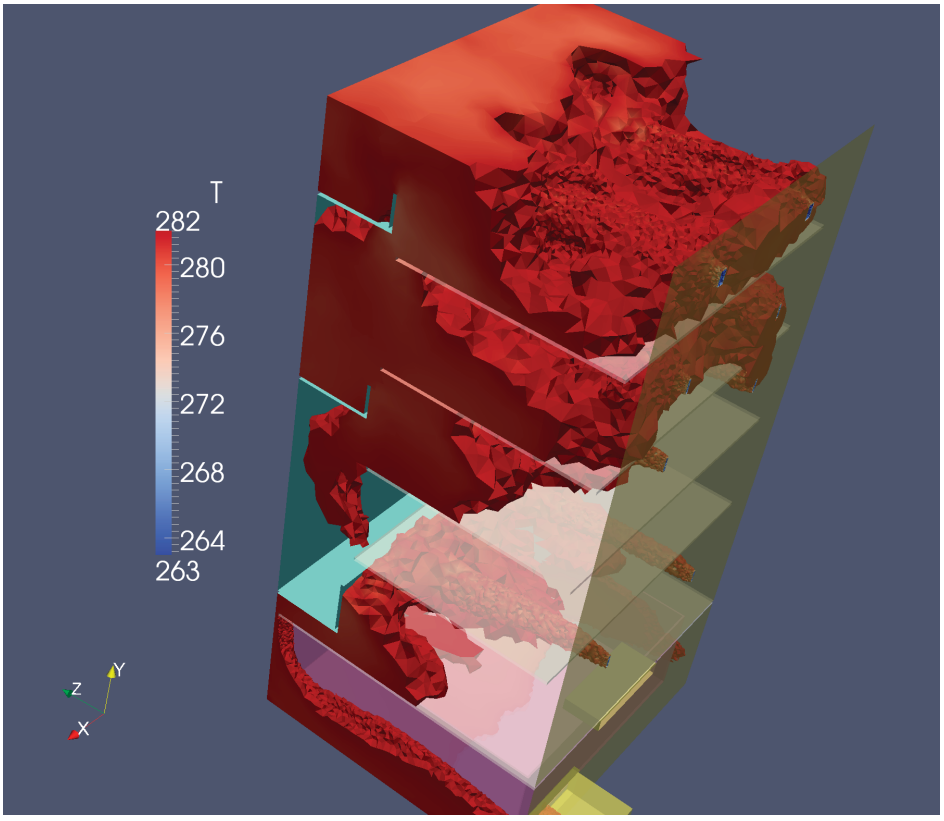

Figure 3: *case*2: Temperature distribution after 15*s* of cooling process starting.

Temperature distribution for *case*1 seen from the back part (section AA') of the refrigerator, after the same 15*s* of simulation, is presented in Figure 4(a). As it can be seen, temperature is not uniform in the horizontal direction, specially in the three upper shelves, where the inlet ports are located. Apart from the inlet jets, the coolest regions are observed near the walls, between second and third shelves. Furthermore, the temperature in the upper part is the lowest, and it increases towards the bottom part of the refrigerating compartment. At this time, all the vegetable compartment remains approximately at the initial temperature for *case*1 configuration. Moreover, the cold air begins to flow down towards the vegetable compartment by the central part of the cabinet in horizontal direction.

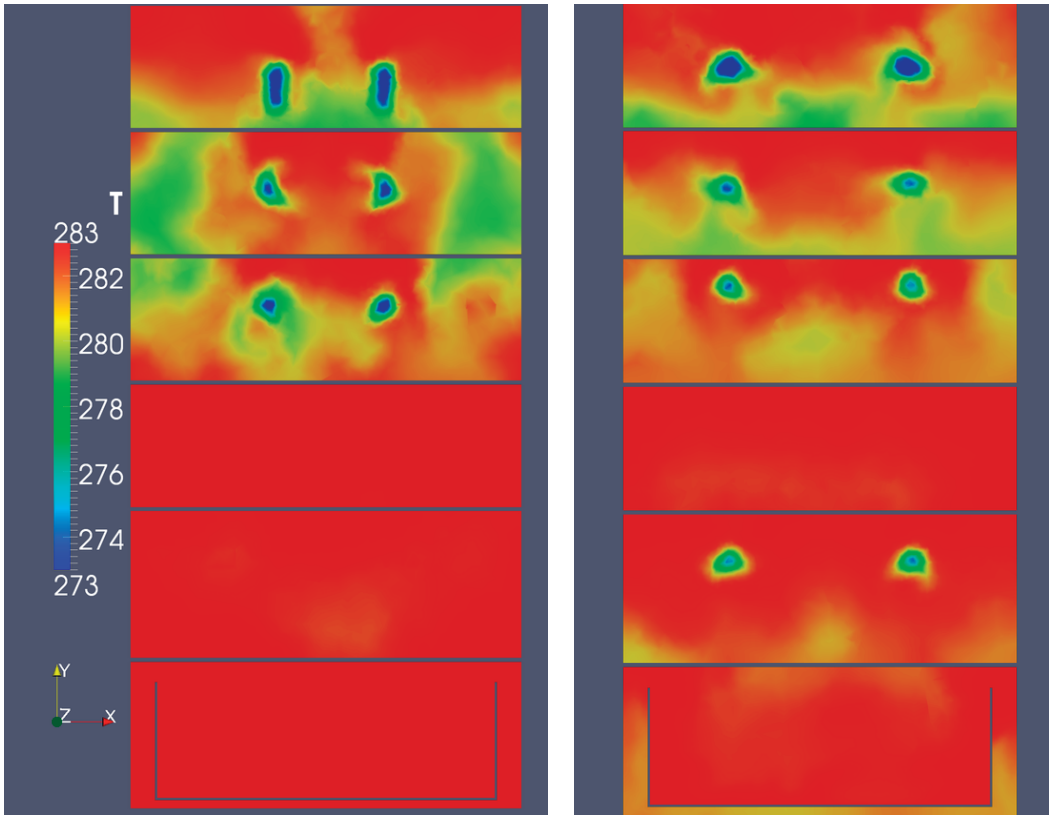

(a) *case*1 (b) *case*2

Figure 4: Temperature distribution in the central cross section AA'.

In order to compare the differences between the inlet configurations studied, a rear view of the temperature distribution for *case*2 (section AA') is shown in Figure 4(b). As it can be seen, in the upper part of the refrigerating cabinet temperature distribution is more regular in horizontal direction. A temperature reduction can be observed over first and second shelves. Using *case*2 temperature profiles are also observable below fourth shelf. Furthermore, now the air flows down more uniformly through the gap between door and cabinet shelves. In this Figure is also possible to observe as the cold air flows around the vegetable box towards the outlet grid reducing in this way temperature in this region, whereas, air within vegetable box remains still almost unchanged.

Figure 5 shows the temperature contours within refrigerating compartment at the symmetry plane BB' for both *case*1 (a) and *case*2 (b). It can be seen from this Figure that using *case*1 the lowest temperature is obtained near the door between the first and second shelves from the top. Hence, a reduction of approximately 7^oC is observed in this zone. Furthermore, in the portion adjacent to the door is where temperature decreases faster. On the other hand, using *case*2 temperature reduction is less than using *case*1, specially in the region near the door. However, a lower temperature is observed in a larger zone within refrigerating compartment. Furthermore, temperature in the region over the trays has reduced more using *case*2, even on the the lid vegetable compartment, and around it. In spite of the temperature reduction using *case*2 is less than using *case*1, a more homogeneous distribution, which covers a larger zone, is obtained. Nevertheless, temperature in the space between third a fourth shelves remains almost unaffected in both *case*1 and *case*2. The addition of the two inlet ports in *case*2 located in the space above the lid of vegetable compartment, as depicted in Figure 1, shows that: i) air on the fifth shelf becomes colder faster than in *case*1, due to the inlets position; ii) the air in the bottom part of the cabinet is colder in *case*2, and it exits colder than in *case*1.

Temperature variations along the central vertical axis are shown in Figure 6. The lowest temperature is observed at $P1$ location and it increases as one moves downward along this axis. For all points studied

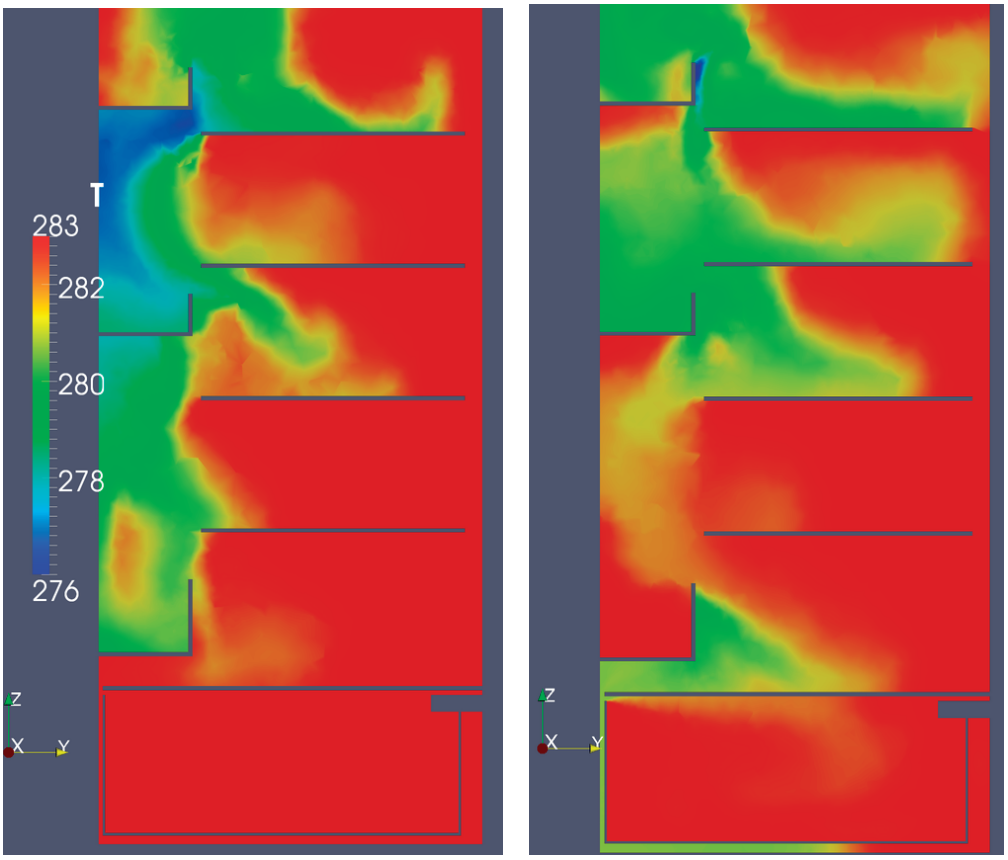

(a) *case*1 (b) *case*2

Figure 5: Temperature distribution on the symmetry central plane BB'.

temperature is lower using *case*2. Moreover, temperature at points $P4$ and $P5$ using *case*1 has not changed. After the first $5s$ of simulation only temperature at $P1$ of *case*2 has decreased considerably. Because of the first cold air impingement against the top door pocket, a recirculation of cold air is created between the two upper inlet jets. Then the air gains heat from surrounding, it becomes warmer and it fills the upper space. In this way a lower temperature at the top shelf is maintained.

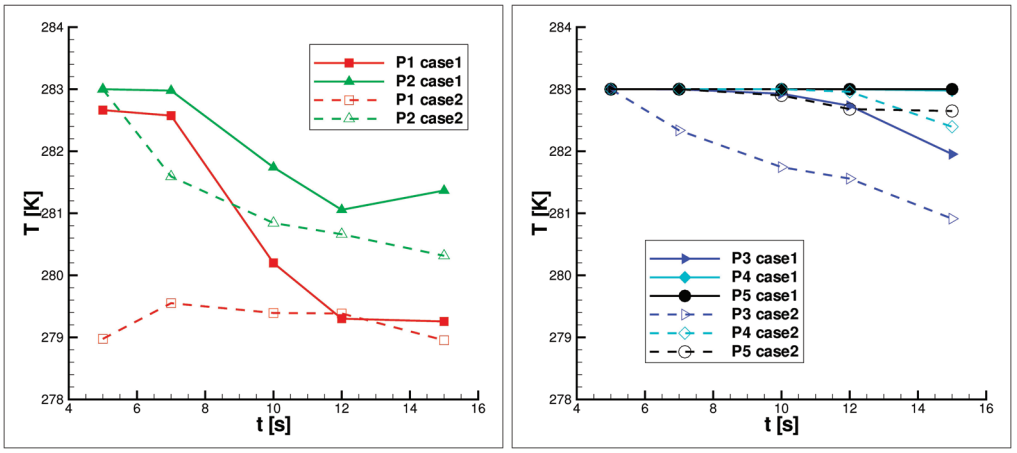

Figure 6: Temperature distribution along the central vertical axis (points $P1$ to $P5$ in Figure 1).

5. CONCLUSIONS

Cases displayed are an example of the versatility and possibilities that numerical simulation provides for the study of refrigerating cabinets of household frost-free refrigerators. Different inlet opening distribution have been studied and their influence on the refrigerator performance evaluated.

Using the proposed inlet ports a more homogeneous temperature distribution in vertical direction is obtained. Furthermore, it is slightly more uniform in the horizontal direction.

With *case*2 configuration a more rapid cooling of larger regions within the refrigerating compartment is observed, i.e. after the same simulation time, the temperature has further decreased. However, it would be interesting to change the position of the two new inlet ports to the space between third and fourth shelves in order to reduce temperature more rapidly in this region.

REFERENCES

Borrell, R., Lehmkuhl, O., Soria, M., and Oliva, A., 2007, Schur complement methods for the solution of Poisson equation with unstructured meshes, *Proceedings of the Parallel CFD 2007 Conference*, p. 1–8.

Ding, G.-L., Qiao, H.-T., and Lu, Z.-L., 2004, Ways to improve thermal uniformity inside a refrigerator, *International Journal of Heat and Mass Transfer*, 24:p. 1827–1840.

Fishpool, G. M. and Leschziner, M. A., 2009, Stability bounds for fractional-step schemes for the Navier-Stokes equations at high Reynolds number, *Computers and Fluids*, 38, no. 6:p. 1289–1298.

Fukuyo, K., Tanaami, T., and Ashida, H., 2003, Thermal uniformity and rapid cooling inside refrigerators, *International Journal of Refrigeration*, 26:p. 249–255.

Gupta, J. K., Gopal, M. R., and Chakraborty, S., 2007, Modeling of a domestic frost-free refrigerator, *International Journal of Refrigeration*, 30:p. 311–322.

Lehmkuhl, O., Perez-Segarra, C. D., Borrell, R., Soria, M., and Oliva, A., 2007, TERMOFLUIDS: A new Parallel unstructured CFD code for the simulation of turbulent industrial problems on low cost PC Cluster, *Proceedings of the Parallel CFD 2007 Conference*, p. 1–8.

Meng, X. and Yu, B., 2009, Experimental research on air flow performance at supply-air openings in frost-free refrigerator by, *Applied Thermal Engineering*, 29:p. 3334–3339.

Nicoud, F. and Ducros, F., 1999, Subgrid-scale stress modeling based on the square of the velocity gradient tensor, *Flow, Turbulence and Combustion*, 62:p. 183–200.

Sagaut, P., 2001, *Large Eddy Simulation for Incompressible Flows*, Springer-Verlag.

Smagorinsky, J., 1963, General circulation experiments with the primitive equations, part. I: the basic experiment, *Monthly Weather Rev.*, 91:p. 99–164.

Verstappen, R. W. C. P. and Veldman, A. E. P., 2003, Symmetry-preserving discretization of turbulent flow, *Journal of Engineering Mathematics*, 187, no. 1:p. 343–368.

ACKNOWLEDGEMENTS

This work has been developed within the collaboration project C07308 between the company Fagor Electrodomésticos, S. Coop. and the Centre Tecnològic de Transferència de Calor (CTTC) of the Universitat Politècnica de Catalunya (UPC).